The Meteoritical Society

Meteoritics & Planetary Science 1–20 (2013)
doi: 10.1111/maps.12171

Nature and degree of aqueous alteration in CM and CI carbonaceous chondrites

Driss TAKIR[1,2*], Joshua P. EMERY[1], Harry Y. McSWEEN Jr.[1], Charles A. HIBBITTS[3], Roger N. CLARK[4], Neil PEARSON[4], and Alian WANG[5]

[1]Department of Earth & Planetary Sciences and Planetary Geosciences Institute, University of Tennessee, Knoxville, Tennessee 37996, USA
[2]Current address: Department of Physics, Ithaca College, Ithaca, New York 14850, USA
[3]Johns Hopkins University Applied Physics Laboratory, Laurel, Maryland 20273, USA
[4]U.S. Geological Survey, Denver, Colorado 80225, USA
[5]Department of Earth and Planetary Sciences and McDonnell Center for Space Sciences, Washington University, St. Louis, Missouri 63130, USA
[*]Corresponding author. E-mail: dtakir@ithaca.edu

(Received 27 December 2012; revision accepted 10 June 2013)

Abstract–We investigated the petrologic, geochemical, and spectral parameters that relate to the type and degree of aqueous alteration in nine CM chondrites and one CI (Ivuna) carbonaceous chondrite. Our underlying hypothesis is that the position and shape of the 3 μm band is diagnostic of phyllosilicate mineralogy. We measured reflectance spectra of the chondrites under dry conditions (elevated temperatures) and vacuum (10^{-8} to 10^{-7} torr) to minimize adsorbed water and mimic the space environment, for subsequent comparison with reflectance spectra of asteroids. We have identified three spectral CM groups in addition to Ivuna. "Group 1," the least altered group as determined from various alteration indices, is characterized by 3 μm band centers at longer wavelengths, and is consistent with cronstedtite (Fe-serpentine). "Group 3," the most altered group, is characterized by 3 μm band centers at shorter wavelengths and is consistent with antigorite (serpentine). "Group 2" is an intermediate group between group 1 and 3. Ivuna exhibits a unique spectrum that is distinct from the CM meteorites and is consistent with lizardite and chrysotile (serpentine). The petrologic and geochemical parameters, which were determined using electron microprobe analyses and microscopic observations, are found to be consistent with the three spectral groups. These results indicate that the distinct parent body aqueous alteration environments experienced by these carbonaceous chondrites can be distinguished using reflectance spectroscopy. High-quality ground-based telescopic observations of Main Belt asteroids can be expected to reveal not just whether an asteroid is hydrated, but also details of the alteration state.

INTRODUCTION

Aqueous alteration is possibly the most widespread process that has affected primitive solar system materials and chondritic meteorites (Brearley 2006). The CM (Mighei-like) and CI (Ivuna-like) carbonaceous chondrites were affected by varying degrees of fluid-assisted alteration (McSween 1979a; Bunch and Chang 1980; Tomeoka and Buseck 1985; Zolensky and McSween 1988; Brearley 2006). Indications of aqueous alteration are obtained from mineralogic (Zolensky et al. 1993; Browning et al. 1996), geochemical (McSween 1979a), oxygen and hydrogen isotopic (Clayton and Mayeda 1999; Eiler and Kitchen 2004), and textural (Lee 1993; Browning et al. 2000) analyses of chondrites.

CM and CI carbonaceous chondrites are widely thought to derive from the C-complex asteroids (Bell et al. 1989; Gaffey et al. 1993). If so, the meteorites and asteroids should have similar mineralogies. Infrared (IR) reflectance spectroscopy of CM and CI chondrites and their possible parent bodies can be useful in identifying hydrated phases, which exhibit a variety of

Table 1. Carbonaceous chondrites analyzed in this study.

Meteorite	Type[c]	Section number	Fall or find[c]	Weathering grade[c]
LAP 02277[a]	CM1	10	Find	A
MIL 07700[a]	CM2	11	Find	A
QUE 97990[a]	CM2	35	Find	BE
QUE 99038[a]	CM2	23	Find	A/B
LAP 03786[a]	CM2	14	Find	A/B
MAC 02606[a]	CM2	7	Find	A
MET 00639[a]	CM2	15	Find	A
Cold Bokkeveld[b]	CM2	182-1	Fall	–
Bells[b]	C2-ung	5293-2	Fall	–
Ivuna[b]	CI1	2478-7413	Fall	–

[a]Sections are from NASA Johnson Space Center (JSC), Houston.
[b]Sections are from the Smithsonian Institution, Washington, DC.
[c]Data from the Meteoritical Bulletin Database.
A = minor rustiness; B = moderate rustiness; E = evaporate minerals visible to the naked eye. (Source: http://curator.jsc.nasa.gov/antmet/amn/weather.htm).

spectral features. For asteroid and meteorite spectroscopy, absorptions around 0.7 and 3.0 μm are particularly diagnostic. The former absorption is attributed to a $Fe^{2+} \rightarrow Fe^{3+}$ charge transfer in phyllosilicates (Vilas and Gaffey 1989), and the latter to hydroxyl- and/or water-bearing materials, or to surficial OH from the solar wind (e.g., Lebofsky 1980; Rivkin et al. 2002; Sunshine et al. 2009).

Laboratory analyses of CM and CI chondrites, coupled with telescopic observations of outer Main Belt asteroids, have the potential to place crucial constraints on how and where this aqueous alteration occurred, and offer a unique insight into the effects of asteroidal processing on early solar system materials. In a previous paper (Takir and Emery 2012), we presented near-infrared (0.7–4.0 μm) spectra of 28 outer Main Belt asteroids. An analysis focused on the 3 μm band in those data revealed four spectral groups, each of which, presumably, is related to distinct surface mineralogy. The goal of the present study is to develop reliable 3 μm spectral indicators that will be used to interpret phyllosilicate mineralogy on the surfaces of these asteroids. To that end, we have undertaken combined petrologic, geochemical, and spectroscopic analyses of selected CM and CI chondrites.

The first part of the investigation consists of a study of the degree of hydration using previously defined alteration parameters (i.e., Mineralogical Alteration Index: MAI, and petrologic subtype) for nine CM carbonaceous chondrites: LaPaz Icefield (LAP) 02277, Miller Range (MIL) 07700, Queen Alexandra Range (QUE) 97990, QUE 99038, LAP 03786, MacAlpine Hills (MAC) 02606, Meteorite Hills (MET) 00639, Cold Bokkeveld, and Bells (Table 1). We apply and compare the previously published alteration scales of Browning et al. (1996) and Rubin et al. (2007), both of which utilized petrographic observations and electron microprobe analyses to quantify the degree of aqueous alteration. The analyses include different splits of the same meteorites previously studied by Browning et al. (1996) and by Rubin et al. (2007) to test the consistency of the two alteration scales. We also compare some results from the XRD-based alteration scale of Howard et al. (2009, 2011) to investigate the consistency of all three aqueous alteration scales, and to identify the most reliable aspects of each scale.

The second part of the investigation evaluates IR reflectance spectral properties (e.g., band centers and shapes) of the same CM chondrites, as well as one CI chondrite (Ivuna). Comparisons of asteroid and meteorite spectra in the 3 μm region have been difficult because meteorite spectra have usually been measured under ambient terrestrial conditions, and therefore were contaminated by atmospheric water (Miyamoto and Zolensky 1994; Sato et al. 1997; Rivkin et al. 2003). Here, we present IR reflectance spectra measured under dry (elevated temperatures) and vacuum (10^{-8} to 10^{-7} torr) conditions to minimize adsorbed water and mimic the space environment, for subsequent comparison with asteroid reflectance spectra. Our reflectance study differs from that of Beck et al. (2010), who measured IR transmission spectra of heated CM and CI chondrites at elevated temperatures up to 575 K. Due to the scattering of reflected illumination by granular particles, the shape and even position of absorption features can differ between transmission and reflectance measurements. Our study is important to investigate the implications of aqueous alteration for outer Main Belt asteroids ($2.5 < a < 4.0$ AU), which are observed in reflectance using ground-based telescopes (Takir and Emery 2012).

METHODOLOGY

Petrologic and Geochemical Analyses of CM and CI Chondrites

Characterization of the 10 CM and CI chondrites included detailed petrographic observations and electron microprobe (EMP) analyses, following procedures outlined by Browning et al. (1996) and Rubin et al. (2007). Polished thin sections were examined with a petrographic microscope, in both transmitted and reflected light. Compositions of matrix material were analyzed with a CAMECA SX-100 electron microprobe at the University of Tennessee, using a 2 μm beam size, 10 nA beam current, and 15 keV accelerating voltage. Counting times for all elements were generally 20–30 s. Standard PAP corrections (Pouchou and Pichoir 1987) were applied. Precision and accuracy were monitored with natural and synthetic standards at intervals during each analytical session, and drift was within counting error. Detection limits (3σ above background) are typically <0.03 wt% for SiO_2, TiO_2, Al_2O_3, MgO, CaO, Na_2O, K_2O, and <0.05 wt% for FeO, MnO, Cr_2O_3, and NiO. We also made multielement X-ray maps of representative regions of the ten carbonaceous chondrites for better characterization of their mineralogy.

Browning et al. Scale

Browning et al. (1996) used petrographic and mineralogic criteria to track the degree of aqueous alteration in CM chondrites. These criteria are based on the relative progress of coupled substitutions in the progressive alteration of Fe-serpentine (cronstedtite) to Mg-serpentine, which increases as alteration advances. This reaction, which defines the Mineralogical Alteration Index (MAI), can be formalized as:

$$2(Fe^{3+}, Al^{3+})_{cronstedtite} = Si^{4+} + (Mg^{2+}, Fe^{2+})_{Mg-serpentine}, \quad (1)$$

where Fe^{3+} atoms occupy tetrahedral and octahedral sites in the idealized serpentine structure.

Browning et al. (1996) proposed two additional indicators of aqueous alteration, the abundance of isolated anhydrous mineral fragments in the matrix and the relative percentage of chondrule alteration. These indicators were based on the assumption that, as alteration proceeds, anhydrous olivine and pyroxene, present as isolated mineral grains in the matrix and within chondrules, progressively alter to serpentine and therefore decrease in abundance. Browning et al. (1996) found correlations between these three indicators of degree of alteration in CM chondrites. The authors also found good correlations between MAI and key bulk properties of CM chondrites, including bulk contents of H and trapped planetary (nonradiogenic) ^{36}Ar. Applying this model to seven CM falls, Browning et al. (1996) established the following relative order of increasing alteration: Murchison ≤ Bells < Pollen ≤ Murray < Nogoya < Mighei < Cold Bokkeveld. Eiler and Kitchen (2004) also found a good correlation between MAI and bulk δD in CM chondrites: MAI increases as δD decreases, except for Murray and Mighei. The hydrogen isotopic change presumably reflects reaction of silicates with an aqueous fluid having a different isotopic composition.

Rubin et al. Scale

Rubin et al. (2007) studied eleven CM chondrites and proposed an alteration sequence that ranges downward from moderately altered petrologic type-2.6 chondrites to highly altered type-2.0 chondrites. This downward numbering scheme reflects the increasing degree of alteration in going from type-3, to type-2, to type-1 carbonaceous chondrites, a reinterpretation (McSween 1979b) of that part of the Van Schmus and Wood (1967) chondrite classification. Rubin et al. (2007) utilized qualitative petrologic observations, including the formation of phyllosilicates, alteration of chondrule mesostases, production of large clumps of serpentine-tochilinite intergrowths, oxidation of metallic Fe-Ni, alteration of mafic silicate phenocrysts in chondrules, changes in tochilinite composition (increase in the phyllosilicate/sulfide ratio), and changes in carbonate mineralogy.

Howard et al. Scale

Howard et al. (2009, 2011) used position sensitive detector X-ray diffraction (PSD-XRD) and X-ray pattern stripping to quantify the modal mineralogy of 13 CM2 and CM1 chondrites. They found a negative correlation between the modal abundances of anhydrous Fe-Mg silicates (olivine and pyroxene) and total phyllosilicates. This variation in modal mineralogy was used as an index of aqueous alteration. An inverse relationship between the abundance of Mg-serpentine and Fe-serpentine suggested that the transition from Fe-rich to Mg-rich serpentine occurs as aqueous alteration progresses.

Visible and Near-Infrared Spectroscopy

Infrared Spectroscopy of Meteorites

Meteorite chips (100–140 mg) were ground into fine powders, using a dry ceramic mortar and pestle. Because we were limited by the sample sizes, we were not able to

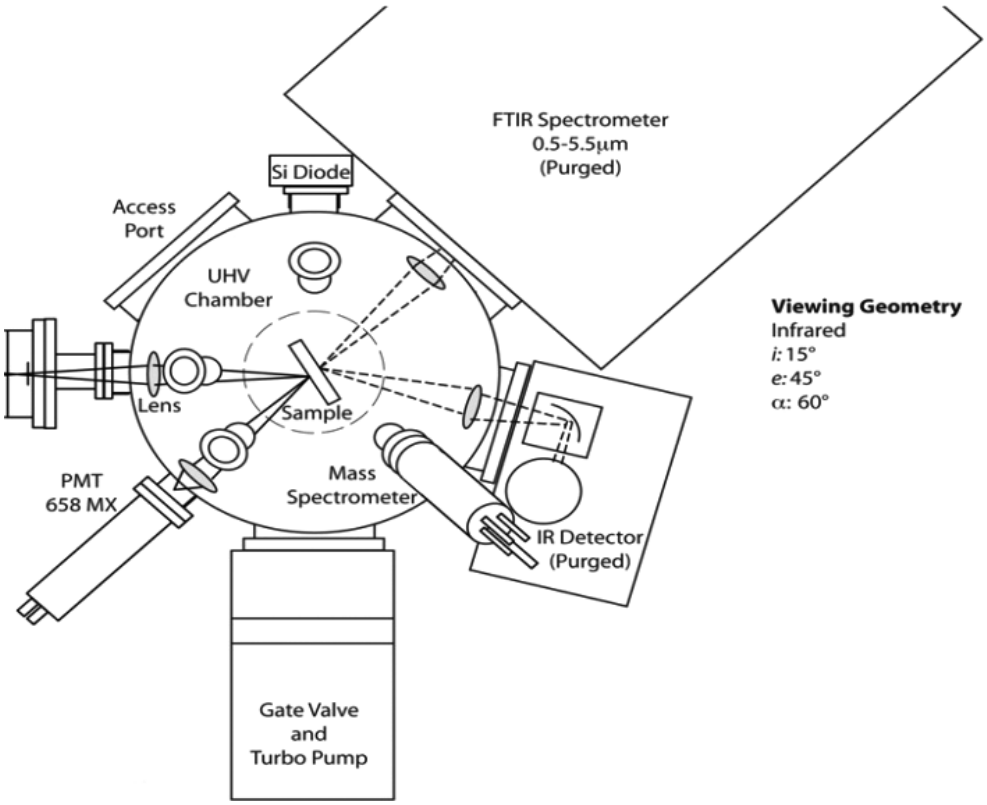

Fig. 1. Optical design of the high-vacuum chamber system with a Bruker Vertex 70 and an external MCT detector used to measure meteorite spectra under dry and vacuum conditions (Hibbitts et al. 2012).

sieve the samples and precisely measure their grain size distributions. IR reflectance spectra of meteorites were measured at the USGS in Denver and the Johns Hopkins University Applied Physics Laboratory (APL) under dry and vacuum conditions. At APL, we collected biconical reflectance spectra ($i = 15°$, $e = 45°$) from approximately 1.7 to 5.5 μm, using a high-vacuum chamber system (10^{-8} to 10^{-7} torr) with a Bruker Vertex 70 spectrometer and an external MCT detector to measure meteorite spectra (Fig. 1). The relative humidity of the chamber was very close to 0. Samples were placed in a copper sample holder that has a $MgFl_2$ window, with powdered anhydrous $MgFl_2$ used as an IR reflectance standard, and a thermocouple (under the window) for accurate temperature measurement. The chamber was sealed and pumped down to 10^{-7}–10^{-8} torr. The meteorite samples were heated to 475 K through a combination of conductive and radiative heating and then cooled to approximately 150 K using liquid N_2 conductive cooling. Spectra were measured in situ during the heating and cooling process.

At USGS, we used a Nicolet Fourier Transform Infrared (FTIR) Interferometer Spectrometer covering the range from approximately 1.3 to 15.5 μm at 4 wavenumber resolution (any use of trade names is for descriptive purposes only and does not constitute endorsement by the authors' institutions). The samples were measured while in a small 15 cm diameter stainless steel environmental chamber through a 5 cm diameter sapphire window. The samples were measured in bidirectional reflectance with an incidence angle of approximately 20°, an emission angle of approximately 35°, and azimuth angle approximately 60°, giving a phase angle of approximately 20°. The entire environmental chamber was heated to 475 K, with temperature measured using an Lakeshore temperature meter with platinum temperature sensor. The environmental chamber, heating stage, optics, and FTIR spectrometer were maintained in a dry nitrogen environment and the sample was held under vacuum, with pressure typically limited by outgassing of the sample as it dehydrated. The samples noticeably shrunk during a dehydration run. We infer that these heating experiments were conducted under asteroid-like conditions. Although there might be some small amounts of adsorbed water present in meteorite powders, this remaining adsorbed water is spectrally insignificant and hence does not affect the 3 μm band in meteorite spectra.

We also used an Analytical Spectral Devices (ASD) portable field spectrometer (model FR) at the

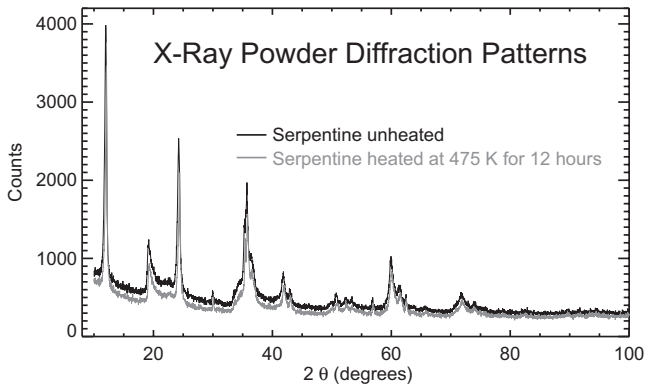

Fig. 2. X-ray powder diffraction patterns of serpentine unheated (black) and heated at 475 K for 12 hours (gray). The similarity of the two diffraction patterns indicates that hydroxyl groups are not affected by modest heating.

University of Tennessee, covering the range from 0.35 to 2.5 μm (hereafter called VNIR spectra) to measure spectra under ambient conditions at an incidence angle (i) of approximately 30° and an emission angle (e) of approximately 30°. The light source of the ASD spectrometer is a quartz-tungsten-halogen bulb. More than 50 VNIR spectra were measured and averaged for each sample. Spectra were measured relative to Spectralon, which has a several percent absorption at approximately 2.13 μm and a blue slope in the 2–2.5 μm region (Weidner and Hsia 1981). Therefore, all VNIR spectra were corrected according to the following equation (Clark et al. 2002):

$$R_{\text{absref}} = \left(\frac{I_{\text{sample}}}{I_{\text{ref}}}\right) R_{\text{ref}}, \tag{2}$$

where R_{absref} is the corrected reflectance, I_{sample} is the light measured by the instrument from the sample, I_{ref} is the light measured by the instrument from the reference under the same incident lighting conditions, and R_{ref} is the absolute reflectance of the reference material (i.e., Spectralon).

Supporting Measurements

To demonstrate that hydroxyl groups remained stable at 450 K, X-ray powder diffraction patterns of serpentine (lizardite) powder unheated and heated at 475 K for 12 hours were obtained. The unheated and heated XRD patterns are quite similar (Fig. 2).

Spectra of serpentine (lizardite) and saponite mixed with carbon black (approximately 1%) were also measured under dry conditions and vacuum to aid interpretation of meteorite spectra. Mixtures of small amounts of spectrally featureless carbon black and clays produce qualitatively similar spectra to those of carbonaceous chondrites in the 3 μm region (Larson et al. 1979; Clark 1983). Serpentine and saponite were obtained from Wards Scientific Co. To characterize additional spectral absorptions in the chondrites, we also measured L-tyrosine amino acid (0.12%) and decane alkane (4%) mixed with Hawaiian Basalt (USGS BHVO-2F, Clark et al., personal communication) under ambient conditions. L-tyrosine amino acid was purchased from Now Foods Co. and labeled as 100% pure. Decane alkane was from Sigma-Aldrich and is 98% pure (Clark et al. 2009). In addition, magnetites in CM and CI chondrites were examined at USGS using a FEI Quanta 450 field emission scanning electron microscope (SEM) in high-vacuum mode at a voltage of 5–20 kV. Backscattered electron images of individual grains were acquired with a voltage contrast detector, and secondary electron images were acquired with an Everhart-Thornley detector.

To provide additional interpretations of meteorite spectra, Raman spectra of powdered CM and CI chondrites (randomly oriented fine grains) were also obtained, using a HoloLab 5000 Raman spectrometer (Kaiser Optical Systems Inc.) at Washington University in St. Louis. The spectrometer uses the 532 nm line of a frequency-doubled Nd:YAG laser for excitation with Stokes-Raman shifted spectral coverage of 50–4300 cm^{-1} and spectral resolution of approximately 4–5 cm^{-1}. Further details on HoloLab 5000 can be found in Wang et al. (2006).

Calculations of Band Parameters

Following a standard technique described by Cloutis et al. (1986), absorption features in the 3, 2.3, and 0.7 μm regions were isolated, and each was divided by a straight-line continuum in wavelength space. The continuum was determined by two maxima at 2.63–2.65 μm and 3.07–3.85 μm for the 3 μm band, by two maxima at 2.20–2.25 μm and 2.35–2.40 μm for the 2.3 μm band, and by two maxima at 0.60–0.65 μm and 0.75–0.85 μm for the 0.7 μm band. For spectra with strong and well-defined features around 3.4–3.5 μm, the continuum for the 3 μm band was determined by two maxima at 2.63–2.65 μm and around 3.3 μm.

The following band parameters were used to analyze spectra of CM and CI chondrites: band centers, band depths, and band areas. The band center was determined by applying a sixth-order polynomial fit to the central part of the feature. Band depth, D_{b}, was calculated using the following equation:

$$D_{\text{b}} = \frac{R_{\text{c}} - R_{\text{b}}}{R_{\text{c}}}, \tag{3}$$

where R_{b} is the reflectance at the band center and R_{c} is the reflectance of the continuum at the band center

Table 2. Estimated chemical formulae of average CM matrix serpentines for nine CM chondrites and Mineralogical Alteration Indices (MAI) of Browning et al. (1996).

	QUE 97990 (n = 6)	MIL 07700 (n = 15)	QUE 99038 (n = 13)	Bells (n = 3)	LAP 03786 (n = 7)	MAC 02609 (n = 2)	Cold Bokkeveld (n = 7)	LAP 02277 (n = 45)	MET 00639 (n = 13)
Si	1.65(0.17)	1.52(0.08)[a]	1.53(0.07)	1.50(0.12)	1.61(0.11)	1.57(0.03)	1.89(0.03)	1.84(0.04)	1.80(0.07)
Al	0.17(0.02)	0.20(0.06)	0.15(0.06)	0.20 (0)	0.17(0.05)	0.15(0.01)	0.13(0.02)	0.15(0.01)	0.16(0.03)
Cr	0.02(0.01)	0.01(0.01)	0.01(0)	0.01 (0)	0.02(0.01)	0.01(0)	0.02(0.01)	0(0)	0.01(0)
Fe^{2+}	0.78(0.31)	0.88(0.23)	0.74(0.08)	0.83 (0.07)	0.77(0.33)	0.73(0.20)	0.72(0.13)	0.71(0.05)	0.87(0.13)
Fe^{3+}	0.52(0.34)	0.76(0.16)	0.78(0)	0.79 (0.25)	0.60(0.17)	0.70(0.07)	0.10(0.01)	0.16(0.08)	0.24(0.14)
Mn	0.01(0)	0.01(0)	0.01(0)	0.01 (0)	0.01(0)	0.01(0)	0.01(0)	0.01(0)	0.01(0)
Mg	1.51(0.24)	1.43(0.29)	1.70(0.05)	1.42 (0.05)	1.56(0.40)	1.57(0.18)	1.92(0.18)	2.09(0.03)	1.73(0.11)
Ca	0.03(0.02)	0.02(0.01)	0.01(0)	0.02 (0.02)	0.03(0.04)	0.05(0.02)	0.02(0.01)	0(0)	0.02(0.02)
Na	0.10(0.03)	0.06(0.02)	0(0)	0.07 (0.02)	0.06(0.02)	0.05(0.01)	0.02(0.01)	0.01(0.01)	0.04(0.01)
Ni	0.07(0.03)	0.02(0.02)	0.02(0.01)	0.05 (0.05)	0.02(0.02)	0.04(0)	0.08(0.03)	0(0)	0.03(0.02)
MAI	0.67(0.48)	0.43(0.13)	0.33(0.09)	0.41 (0.11)	0.45(0.08)	0.35(0.04)	1.21(0.32)	1.04(0.31)	0.90(0.33)

[a]Numbers in parentheses correspond to 2σ standard deviations that represent the range of matrix serpentine compositions in the nine CM chondrites.

(Clark and Roush 1984). The band area was calculated by integrating the spectral curve below the straight-line continuum. An average of five measurements, determined by varying the positions of band maxima, was used for each band parameter. Uncertainty for each parameter was determined by the 2σ standard deviation that represents variability from the average. The band depths at 2.80 and 2.72 μm were calculated relative to the continuum that is defined as the regression line across the 1.95–2.50 μm region (Takir and Emery 2012).

RESULTS

Petrologic and Geochemical Properties

Browning et al. Scale

Applying the previously published scale of Browning et al. (1996), we determined the MAI for the nine CM chondrites. Table 2 shows the estimated chemical formulae of average matrix serpentines and MAI for the CM chondrites analyzed in this study. The reported MAI is the average of MAIs for the matrix analyses in an individual CM chondrite. Standard deviations for each cation do not represent analytical errors, but illustrate the compositional variability of matrix serpentines. Atomic formulae were determined from microprobe analyses, which were corrected for small amounts of sulfide, following the algorithm outlined in Browning et al. (1996).

Rubin et al. Scale

We also applied the previously published scale of Rubin et al. (2007). Tables 3 and 4 summarize our results on various petrologic properties, including oxidation of metallic Fe-Ni, alteration of chondrule phenocrysts, changes in tochilinite compositions, and carbonate mineralogy. Using the criteria outlined by Rubin et al. (2007), petrologic subtypes (±0.1) were assigned to the nine CM chondrites. The petrologic subtypes vary between 2.6 and 2.1, representing the least altered and most altered chondrites, respectively. The aqueous alteration scales of Browning et al. (1996) and Rubin et al. (2007) for the same chondrites weakly correlate with each other, and where XRD data on the same meteorites are available, also with the scale of Howard et al. (2009, 2011) (Fig. 3).

Spectral Properties of CM and CI Chondrites

Figures 4a–j show IR reflectance spectra of nine CM chondrites and one CI chondrite measured at ambient, and at dry and vacuum conditions. All spectra exhibit an apparent 3 μm band. Some spectra also show a very weak absorption feature at approximately 2.3 μm with band depth less than 1%. The 3 μm band center shifts to shorter wavelengths under dry conditions for some samples, mainly due to the removal of adsorbed water.

Figure 5 illustrates red-sloped VNIR spectra of these CM and CI chondrites. A few VNIR spectra exhibit a very weak 0.7 μm absorption feature with a band depth less than 1%. QUE 99038 and MIL 07700 exhibit 1 and 2 μm features and no 2.3 μm feature. Ivuna's VNIR spectrum shows a shoulder at approximately 0.6 μm, an overall red slope between 0.4 and 2.3 μm, and an absorption feature at approximately 1.9 μm. Tables 5a and 5b include the 3,

Table 3. Tochilinite compositions (wt%) in CM chondrites.

	QUE 97990 (n = 26)	MIL 07700 (n = 47)	QUE 99038 (n = 14)	Bells (n = 10)	LAP 03786 (n = 60)	MAC 02609 (n = 8)	Cold Bokkeveld (n = 14)	LAP 02277 (n = 8)	MET 00639 (n = 23)
SiO_2	19.7(23)	25.6(13)[a]	28.3(16)	25.8(49)	25.7(27)	30.4(35)	22.8(92)	28.2(23)	24.2(34)
TiO_2	0.04(2)	0.07(02)	0.16(12)	0.06(3)	0.29(33)	0.10(4)	0.09(3)	0.79(16)	0.06(04)
Al_2O_3	3.05(57)	2.63(23)	3.03(73)	4.00(63)	2.50(48)	2.22(24)	3.14(26)	1.89(49)	2.19(56)
"FeO"	51.9(59)	31.6(30)	34.6(23)	34.6(75)	28.5(53)	26.4(57)	34.7(81)	26.2(33)	38.3(55)
Cr_2O_3	0.08(8)	0.29(6)	0.40(16)	0.28(11)	0.26(15)	0.53(18)	0.87(95)	0.48(22)	0.24(7)
MnO	0.18(3)	0.21(3)	0.20(2)	0.16(6)	0.22(5)	0.21(6)	0.22(3)	0.23(3)	0.19(4)
MgO	7.91(52)	17.2(18)	20.9(12)	15.2(50)	15.7(30)	17.0(15)	12.5(55)	18.6(63)	16.8(25)
CaO	0.19(13)	0.46(38)	0.10(4)	0.84(27)	0.77(52)	0.73(26)	0.86(82)	4.18(23)	0.14(11)
Na_2O	0.50(29)	0.53(9)	0.05(3)	0.38(24)	0.70(32)	0.55(10)	0.20(13)	0.10(5)	0.28(6)
K_2O	0.06(4)	0.05(2)	0.02(2)	0.09(4)	0.04(6)	0.09(3)	0.09(4)	0.02(1)	0.02(2)
P_2O_5	0.02(2)	0.14(23)	0.24(6)	0.11(3)	0.31(93)	0.05(4)	0.67(66)	0.08(15)	0.02(6)
NiO	0.81(52)	1.24(45)	0.60(16)	1.49(11)	1.30(16)	1.30(58)	3.25(99)	3.52(98)	1.47(54)
S	3.13(4)	2.82(55)	0.28(11)	2.64(75)	2.58(4)	4.41(45)	2.11(72)	6.52(85)	5.06(67)
Total	86.76	81.96	88.83	85.02	78.32	82.90	80.84	89.13	87.76
S/SiO_2	0.17	0.11	0.01	0.11	0.10	0.15	0.17	0.23	0.22
"FeO"/SiO_2	2.70	1.23	1.23	1.43	1.13	0.89	1.59	0.94	1.63

[a]Numbers in parentheses correspond to 1σ standard deviations from the mean in terms of least units cited.
The "FeO" concentration includes FeO in phyllosilicates, Fe^{3+} in cronstedtite, and Fe^{2+} in sulfide.

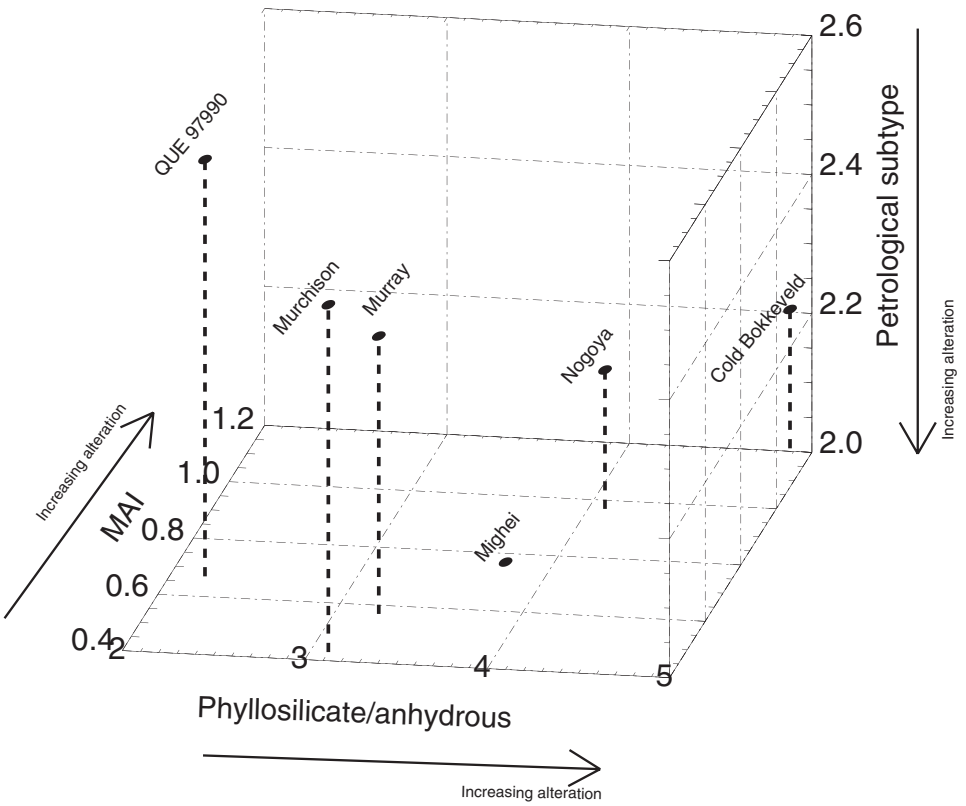

Fig. 3. A 3-D plot comparing the results of three alteration scales. The x-, y-, and z-axes represent the Howard, Browning, and Rubin scales, respectively. The plot includes samples analyzed by Browning et al. (1996), Rubin et al. (2007), and Howard et al. (2009, 2011). The plot includes two samples (QUE 97990 and Cold Bokkeveld) that were also analyzed by Rubin et al. (2007) and Howard et al. (2009, 2011). Mighei was not part of the Rubin et al. (2007) sample, nor of the current work.

Table 4. Diagnostic characteristics of progressive alteration in CM chondrite petrologic subtypes of Rubin et al. (2007).

	QUE 97990	MIL 07700	QUE 99038	Bells	LAP 03786	MAC 02606	Cold Bokkeveld	LAP 02277	MET 00639
Chondrule mesostasis	Phyllosilicate	Phyllosilicate	Phyllosilicate	Phyllosilicate	Phyllosilicate	Phyllosilicate	Phyllosilicate	Phyllosilicate	Phyllosilicate
Matrix phyllosilicates	Abundant	Abundant	Abundant	Abundant	Abundant	Abundant	Abundant	Abundant	Abundant
Metallic Fe-Ni	1 vol%	0.03–0.3 vol%	0.03–0.3 vol%	≤ 0.02 vol%	0.03–0.3 vol%	≤ 0.02 vol%	0.03–0.3 vol%	≤ 0.02 vol%	0.03–0.3 vol%
Mafic silicate phenocrysts in chondrules	Unaltered	2–15 vol% altered	Unaltered	85–99 vol% altered	15–85 vol% altered	85–99 vol% altered	15–85 vol% altered	85–99 vol% altered	15–85 vol% altered
Large PCP clumps	15–40 vol%	15–40 vol%	15–40 vol%	2–5 vol%	15–40 vol%	2–5 vol%	15–40 vol%	2–5 vol%	15–40 vol%
PCP compositions: "FeO"/SiO_2	2.70	1.23	1.23	1.13	1.43	0.89	1.59	0.94	1.63
Sulfide	po + pn	po + pn	po + pn	po + pn	po + pn	po + pn	po + pn	po + pn	po + pn
Carbonate	Ca	Ca	Ca	Ca & complex	Ca	Ca & complex	Ca	Ca	Ca
Petrologic subtype	2.6	2.3	2.4	2.1	2.2	2.1	2.2	2.1	2.2

The "FeO" concentration includes FeO in phyllosilicates, Fe^{3+} in cronstedtite, and Fe^{2+}in sulfide; po = pyrrhotite; pn = pentlandite.

Table 5a. The 3 μm feature parameters for meteorite spectra measured in dry conditions and the 2.3 and 0.7 μm parameters for meteorite spectra measured in ambient conditions.

	3 μm Band			2.3 μm Band		0.7 μm Band		
	Center (μm)	Depth (%)	Area(μm^{-1})	Center (μm)	Depth (%)	Center (μm)	Depth (%)	Ratio[a]
QUE 97990	2.796 ± 0.001	31.95 ± 0.91	0.10 ± 0.03	2.31 ± 0.002	0.46 ± 0.17	0.732 ± 0.014	0.73 ± 0.23	0.83
MIL 00770	2.784 ± 0.001	4.52 ± 0.13	0.01 ± 0.01	n.d	n.d	n.d	n.d	0.97
QUE 99038	2.773 ± 0.010	16.85 ± 0.49	0.11 ± 0.01	n.d	n.d	n.d	n.d	0.97
Bells	2.778 ± 0.002	41.88 ± 0.71	0.15 ± 0.03	2.299 ± 0.004	0.39 ± 0.15	0.738 ± 0.003	1.36 ± 0.44	0.95
LAP 03786	2.775 ± 0.001	39.58 ± 0.22	0.12 ± 0.01	2.328 ± 0.005	0.49 ± 0.10	0.730 ± 0.005	0.60 ± 0.18	0.92
MAC 02606	2.770 ± 0.006	16.16 ± 0.37	0.04 ± 0.01	2.311 ± 0.009	0.48 ± 0.05	n.d	n.d	0.99
Cold Bokkeveld	2.759 ± 0.003	32.73 ± 0.28	0.09 ± 0.01	2.319 ± 0.001	0.51 ± 0.08	n.d	n.d	0.97
LAP 02277	2.723 ± 0.001	31.77 ± 0.45	0.05 ± 0.01	2.306 ± 0.025	0.62 ± 0.22	0.727 ± 0.001	1.63 ± 0.25	1.11
MET 00639	2.722 ± 0.001	17.78 ± 0.39	0.02 ± 0.01	n.d	n.d	n.d	n.d	1.08
Ivuna	2.715 ± 0.001	40.71 ± 0.15	0.06 ± 0.01	2.316 ± 0.003	0.67 ± 0.08	n.d	n.d	1.25

n.d. = not detected.
Uncertainty for each parameter was determined by the 2σ standard deviation that represents variability from the average.
[a]Ratio of the 2.8 μm band depth to the 2.72 μm band depth.

Table 5b. The 3 μm feature parameters for cronstedtite, the three Mg-serpentine polymorphs, and saponite.

	3 μm Band center (μm)	2.3 μm Band center (μm)
Cronstedtite[a]	2.852 ± 0.002	2.327 ± 0.002
Antigorite[b]	2.720 ± 0.001	2.316 ± 0.001
Lizardite[b]	2.713 ± 0.001	2.331 ± 0.003
Chrysotile[b]	2.710 ± 0.001	2.300 ± 0.016
Saponite (dry)	2.722 ± 0.001	2.328 ± 0.006
Lizardite (dry)	2.711 ± 0.015	2.326 ± 0.003

Uncertainty for each parameter was determined by the 2σ standard deviation that represents variability from the average.
[a]Spectrum from Clark et al. (2007) measured at ambient conditions with a strong adsorbed water feature.
[b]Spectra from Salisbury et al. (1991) measured at ambient conditions.

2.3, and 0.7 μm band centers and depths for these chondrites and additional minerals, respectively.

DISCUSSION

Mineralogical Alteration Index

Velbel and Palmer (2012) suggested that the application of the MAI is problematic because it includes Al, which is not a good indicator of aqueous alteration in CM chondrites. According to these authors, the main problems with the MAI are mathematical, as division by zero occurs where Si obtains its stoichiometric value of 2 in pure serpentine, and by the biases caused by data screening. Under certain circumstances, these potential problems could result in very large values of MAI (greater than 2), leading to the elimination of valid phyllosilicate analyses.

We were able to apply the MAI to the nine CM chondrites without encountering any of the problems raised by Velbel and Palmer (2012). After reducing electron microprobe data of the matrices in CM chondrites, following the procedure described by Browning et al. (1996), all calculated Si cations were found to be far less than 2 (Table 2). For CM chondrites, experience indicates that it is unrealistic to expect pure serpentine with a Si cation of value 2 (Zolensky et al. 1993). Data screening, as outlined by Browning et al. (1996), is necessary to exclude cation totals that are representative of nonserpentine phyllosilicates, carbonates, and oxides. The expression used by Browning et al. (1996) to determine the amount of Fe^{3+},

$$Fe^{3+} = (2 * (2 - Si)) - Al, \quad (4)$$

remains valid, assuming a loss of Si is accommodated by coupled substitutions that deplete all the available Al. Moreover, Fig. 9 in Velbel and Palmer (2012) shows an extremely weak correlation ($R^2 = 0.09$) between the chemical index of alteration (CIA) and Si/Al ratio, making it difficult to draw any conclusion about the mobility of Si relative to Al during leaching of CMs. Therefore, the criticisms raised by Velbel and Palmer (2012) have not convinced us to abandon the application of the Browning et al. (1996) scale, as applied specifically to CM chondrites. We also note that there is a typographical error in Table 2 of Browning

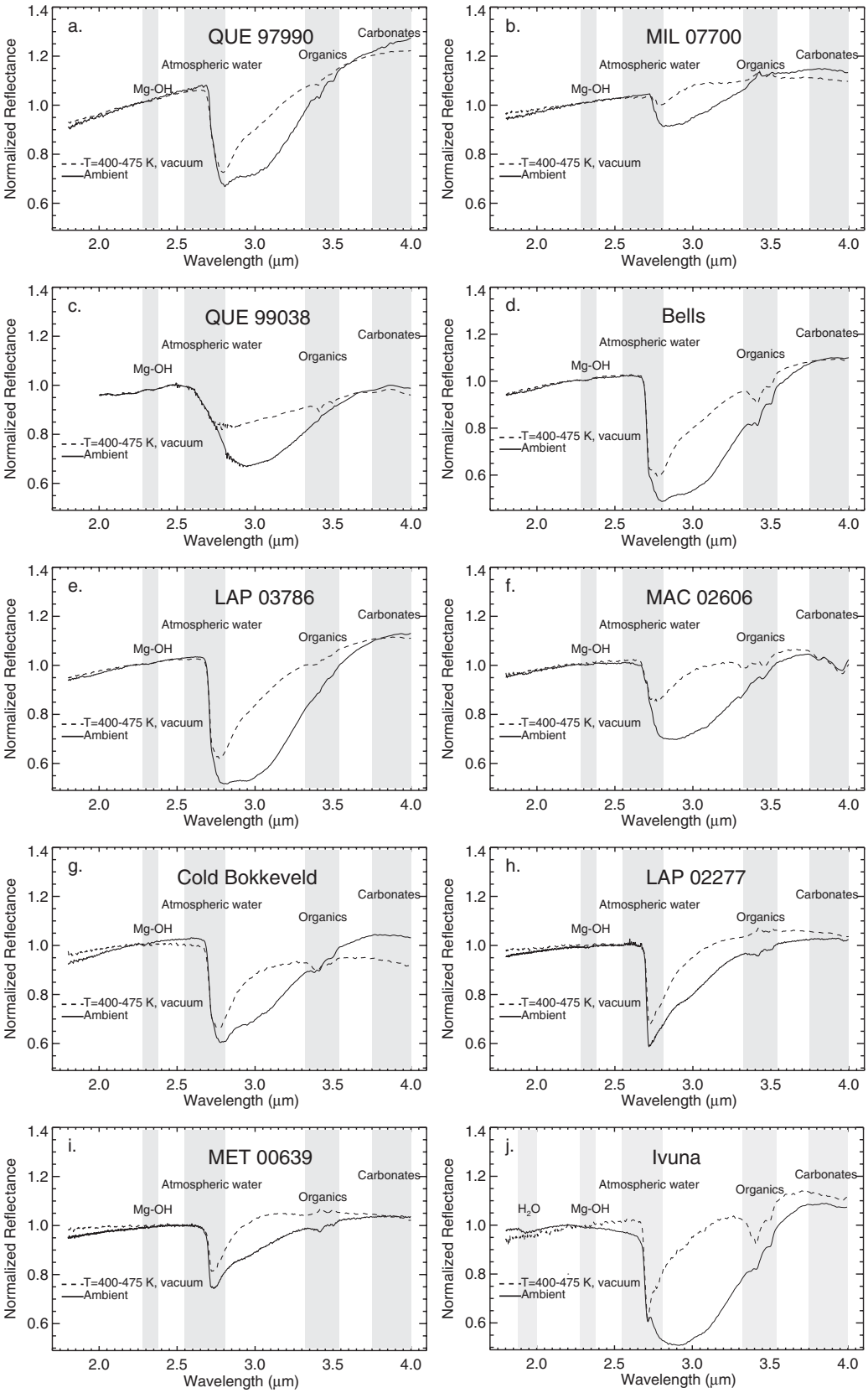
a.
QUE 97990
b.
MIL 07700
c.
QUE 99038
d.
Bells
e.
LAP 03786
f.
MAC 02606
g.
Cold Bokkeveld
h.
LAP 02277
i.
MET 00639
j.
Ivuna
Atmospheric water
Organics
Carbonates
Mg-OH
H2O
T=400-475 K, vacuum
Ambient
Normalized Reflectance
Wavelength (μm)

Fig. 4. a-j. Average IR reflectance spectra of CM and CI chondrites measured at ambient (solid curves), and dry and vacuum conditions (dashed curves). Several spectra were averaged for each temperature and pressure step. The atmospheric water bar in the figures marks the region of strong absorption by water vapor in Earth's atmosphere in which we cannot observe asteroids. Note the significant spectral effect of adsorbed water for the sample measured under ambient conditions. All spectra have been normalized to unity at 2.2 μm. See the supporting information for plots of spectra during the entire heating and depressurization sequence. Except for spectra of QUE 99038, which were measured at USGS, all other spectra were measured at APL.

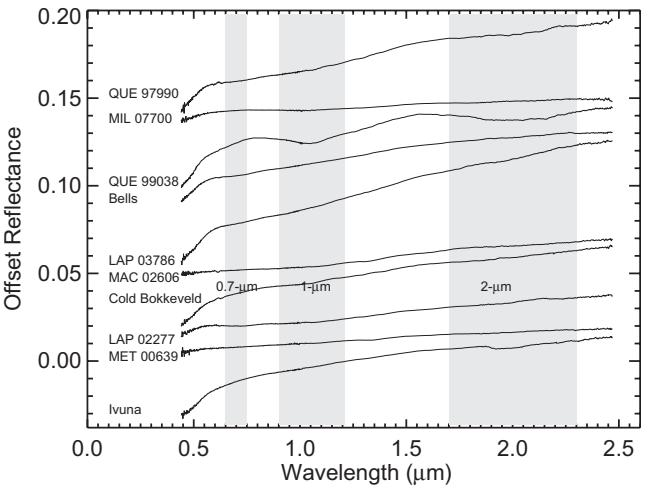

Fig. 5. VNIR reflectance spectra of CM and CI carbonaceous chondrites. Some spectra show a very weak 0.7 μm feature (band depth less than 1%), and 1 and 2 μm features.

et al. (1996); the MAIs listed in column 12 should be subtracted from 2 because the MAI is defined as:

$$\mathrm{MAI} = 2 - \frac{\mathrm{Fe}^{3+}}{2 - \mathrm{Si}}. \quad (5)$$

Diversity in the 3 μm Band in CM and CI Chondrites

CM and CI chondrites display three distinct types of spectra. This spectral classification is generally not affected by the grain size distribution of the samples because spectra are mainly distinguished by the 3 μm band center. "Group 1," that includes QUE 97990, MIL 00700, and QUE 99038, possesses a 3 μm band centered at approximately 2.77–2.80 μm (Figs. 4a–c). "Group 2" includes Bells, LAP 03786, MAC 02606, and Cold Bokkeveld. This group has a 3 μm band centered at approximately 2.76–2.78 μm, with a shoulder near approximately 2.72 μm (Figs. 4d–g). "Group 3," which includes LAP 02277 and MET 00639, exhibits a 3 μm band centered at approximately 2.72 μm (Figs. 4h-i). The band centers for all meteorites and minerals used in this study are listed in Tables 5a and 5b, respectively. The diversity in the 3 μm band in CM and CI chondrites is further supported by calculation of the ratio of the band depth at 2.80 μm to the band depth at 2.72 μm (Table 5a, column 8). Except for MIL 07700 and QUE 99038, which are olivine- and pyroxene-rich chondrites (less altered), it appears that there is a trend between the ratio and the meteorite spectral groups.

Spectral Interpretations

Spectra of group 1 exhibit 3 μm band centers that are at longer wavelengths than most serpentines or some smectites (e.g., saponite), the matrix mineral compositions commonly discussed for CM matrices. The longer wavelength band center is, however, consistent with cronstedtite (Fig. 6a), a serpentine for which Fe^{3+} replaces some Si in the tetrahedral site. Two group 1 meteorites, QUE 99038 and MIL 00770, exhibit absorptions at approximately 1 and 2 μm, attributed to Fe^{2+} in the M2 crystallographic site in olivine and pyroxene (Burns 1993) (Fig. 6b), indicating a high fraction of anhydrous silicates in these samples. Raman spectra confirm the high concentrations of olivine in QUE 99038 (Fig. 6c).

Group 2 samples show a particularly strong 3.1 μm feature in ambient spectra, attributed to adsorbed water. This feature goes away as the sample is desiccated in vacuum at elevated temperatures. In addition, dry spectra of this group exhibit a 3.4–3.5 μm feature, attributed to C-H stretching of aliphatic organic compounds (Clark et al. 2009). The organics features become sharper as heating proceeds. MAC 02606 has a unique spectrum in that it exhibits strong CO_3 absorptions in the 3.4–3.5 μm and 3.8–4.0 μm regions, attributed to carbonates (Clark et al. 2007) (Fig. 6d). Carbonates were also detected in MAC 02606, using multielement X-ray maps and microprobe analyses. Raman spectra show that the carbonate in this sample is dominated by dolomite (Fig. 6e). All samples in group 2 also exhibit a 2.3 μm feature usually, but not uniquely, attributed to Mg-OH stretching (Clark et al. 1990). The 2.3 μm feature was not affected by heating the samples, providing additional confidence that the structural OH was not altered.

Spectra of group 3 exhibit band centers and shapes that are more consistent with typical serpentines. In particular, the band position of the serpentine antigorite matches that of the two group 3 meteorites (Fig. 6f). Ambient spectra of this group do exhibit a much weaker 3.1 μm feature (attributed to adsorbed water)

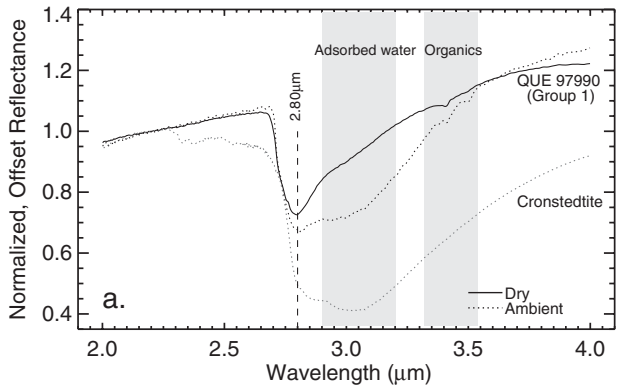
Normalized, Offset Reflectance
Adsorbed water
Organics
2.80μm
QUE 97990
(Group 1)
Cronstedtite
Dry
Ambient
a.
Wavelength (μm)

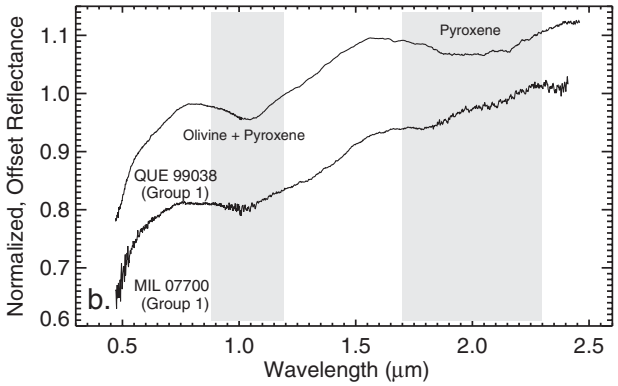
Normalized, Offset Reflectance
Pyroxene
Olivine + Pyroxene
QUE 99038
(Group 1)
MIL 07700
(Group 1)
b.
Wavelength (μm)

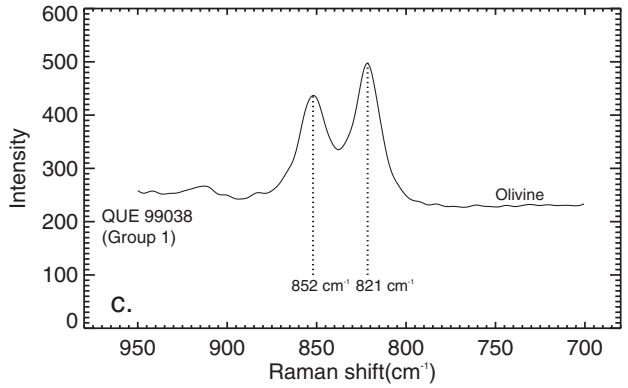
Intensity
QUE 99038
(Group 1)
Olivine
852 cm-1 821 cm-1
c.
Raman shift(cm-1)

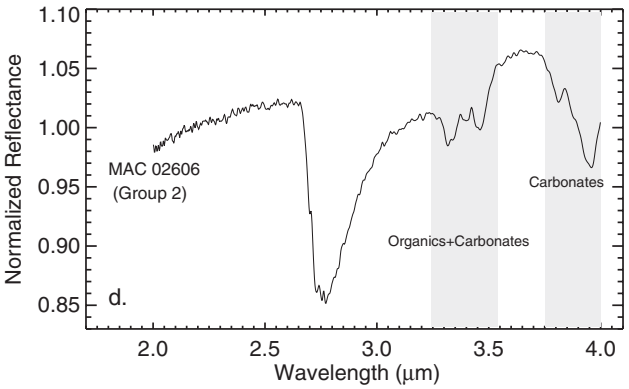
Normalized Reflectance
MAC 02606
(Group 2)
Carbonates
Organics+Carbonates
d.
Wavelength (μm)

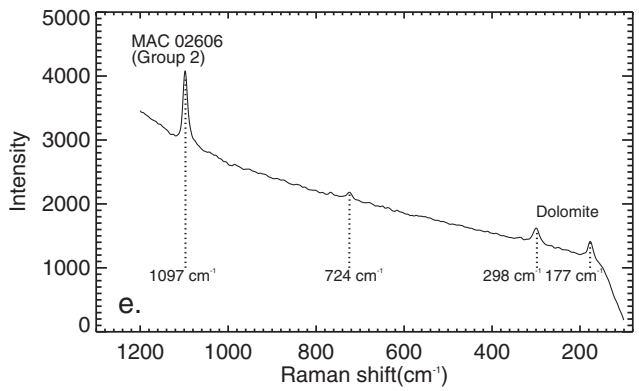
Intensity
MAC 02606
(Group 2)
Dolomite
1097 cm-1
724 cm-1
298 cm-1
177 cm-1
e.
Raman shift(cm-1)

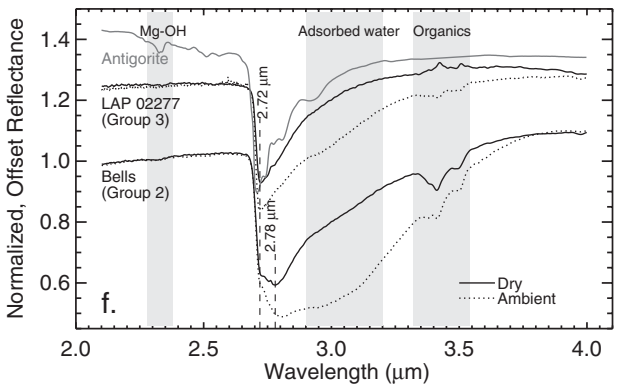
Normalized, Offset Reflectance
Mg-OH
Adsorbed water
Organics
Antigorite
LAP 02277
(Group 3)
Bells
(Group 2)
2.72 μm
2.78 μm
Dry
Ambient
f.
Wavelength (μm)

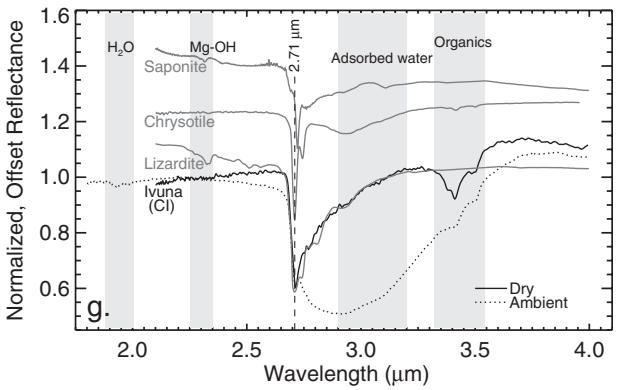
Normalized, Offset Reflectance
H2O
Mg-OH
Saponite
2.71 μm
Adsorbed water
Organics
Chrysotile
Lizardite
Ivuna
(CI)
Dry
Ambient
g.
Wavelength (μm)

Fig. 6. a) Spectrum of QUE 99790 (group 1) is consistent with cronstedtite, both measured at ambient conditions. The cronstedtite spectrum is from the USGS spectral library (Clark et al. 2007) and is affected by a strong adsorbed water feature. b) Silicate-rich QUE 99038 and MIL 00770, which exhibit absorptions at approximately 1 and 2 μm in VNIR spectra, attributed to olivine and pyroxene. c) Raman spectrum also shows olivine in QUE 99038. d) MAC 02606 (group 2) exhibits unique strong CO_3 absorptions in the 3.4–3.5 μm and 3.8–4.0 μm regions. e) Raman spectrum shows that the type of carbonate in MAC 02606 is dolomite. f) Group 2, which includes Bells, is distinguishable by a 3 μm band center that varies from 2.76 to 2.80 μm. This group is also distinguishable by ambient spectra that exhibit a broad feature at approximately 3.1 μm, attributed to adsorbed water, which is minimized at dry conditions and vacuum. Group 3, which includes LAP 02277, is distinguishable by a narrower and shallower 3 μm band centered at approximately 2.72 μm, consistent with serpentine (antigorite). g) Ivuna, the only CI chondrite analyzed in the present study, is distinct from all of the CM groups, with a very narrow 3 μm band centered at approximately 2.71 μm, consistent with lizardite and chrysotile and not saponite. Ivuna also exhibits a distinctive water feature at approximately 1.9 μm, which goes away at elevated temperatures and vacuum as adsorbed water is minimized from the sample.

than the other groups. Dry spectra of this group do not show any indications of organic features at 3.4–3.5 μm.

Ivuna, which is the only CI chondrite included in the present study, is distinct from all of the CM groups, with a 3 μm band centered at approximately 2.71 μm that is consistent with serpentine (lizardite and chrysotile) (Fig. 6g). Ivuna is also unique because it exhibits a distinctive water feature at approximately 1.9 μm, which becomes weaker as the sample is desiccated. Osawa et al. (2005) also reported that Ivuna and another CI chondrite, Orgueil, exhibit a narrow feature at approximately 2.71 μm, under ambient conditions. They attributed this feature to serpentine (lizardite) rather than saponite. However, Zaikowski (1979) attributed the 2.71 μm feature in Orgueil, also under ambient conditions, to chlorite and chamosite rather than serpentine or saponite. Although minor phyllosilicates other than serpentine are also present in CM and CI chondrites (Brearley 2006), these sparse phyllosilicates are spectrally insignificant.

Geochemical Analyses

Figure 7, a ternary diagram of SiO_2+Al_2O_3, FeO, and MgO, compares our analyzed matrix compositions in CM chondrites and Ivuna. The matrix compositions lie along an approximately linear trend that extends from near the composition of cronstedtite (representing the least altered material) toward the SiO_2-MgO join near the composition of Mg-serpentine (representing the most altered material). This trend is typical for carbonaceous chondrites (e.g., Brearley 1997). The matrix composition of QUE 97990, which is assigned to subtype 2.6, plots near cronstedtite in agreement with the spectral analysis, providing more evidence that this meteorite is the least altered sample in the present study. The matrix compositions of CM and CI chondrites plot along the cronstedtite-serpentine join far from saponite, vermiculite, and montmorillonite, suggesting that the former mineral is more abundant in these chondrites in agreement with the spectroscopic investigation. Although these geochemical analyses generally support our spectral investigation and alteration sequence, they do not uniquely distinguish the spectral classes identified in CM and CI chondrites.

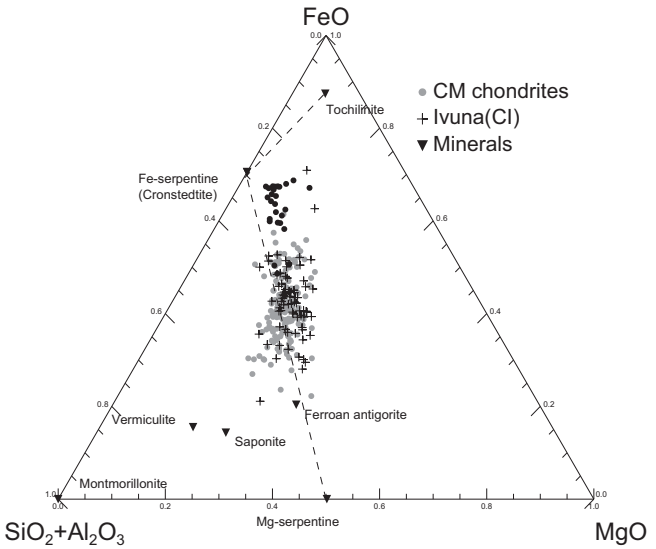

Fig. 7. SiO_2+Al_2O_3-FeO-MgO diagram showing matrix compositions of CM chondrites and Ivuna, as well as some alteration minerals: serpentine—$Mg_3Si_2O_5(OH)_4$, montmorillonite—$(Na,Ca)_{0.3}(Al,Mg)_2Si_4O_{10}(OH)_2{\bullet}n(H_2O)$, vermiculite—$(Mg,Fe^{2+},Al)_3(Al,Si)_4O_{10}(OH)_2{\bullet}4(H_2O)$, $(Ca/2,Na)_{0.3}(Mg,Fe^{2+})_3(Si,Al)_4O_{10}(OH)_2{\bullet}4(H_2O)$ "$Fe_2^{2+}Fe^{3+}(SiFe^{3+})O_5(OH)_4$" ferroan antigorite—$(Mg,Fe^{2+})_3Si_2O_5(OH)_4$, and cronstedtite—$Fe^{2+}{}_2Fe^{3+}(SiFe^{3+})O_5(OH)_4$. Tochilinite data are from Tomeoka and Buseck (1985). The matrix compositions lie along an approximately linear trend that extends from near the composition of cronstedtite (representing the least altered material) toward the SiO_2-MgO join near the composition of Mg-serpentine (representing the most altered material). The black filled circles are from QUE 97990 (the least altered sample in the present study). See the supporting information for more diagrams of matrix compositions of CM chondrites and Ivuna.

Alteration Parameters and Spectral Properties of CM Chondrites

Figure 8 summarizes the results of the petrologic, geochemical, and spectral investigation of the CM chondrites and Ivuna. Group 1 is the least altered

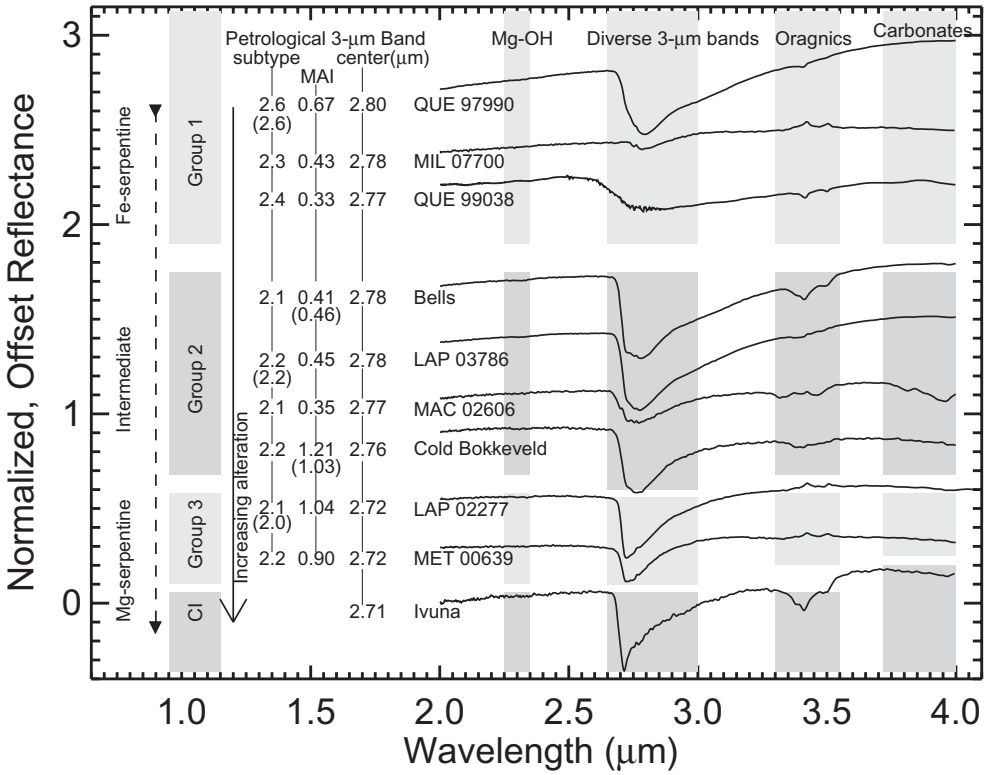

Fig. 8. IR reflectance spectra of CM and CI carbonaceous chondrites measured under dry and vacuum conditions. The MAI and the petrologic subtype were determined applying the alteration scales of Browning et al. (1996) and Rubin et al. (2007), respectively. The MAI and petrologic subtype values in parentheses are from Browning et al. (1996) and Rubin et al. (2007), respectively. Our spectral investigation revealed distinct groups among CM chondrites: group 1 (QUE 97990, QUE 99038, and MIL 07700), group 2 (Bells, LAP 03786, MAC 02606, and Cold Bokkeveld), and group 3 (LAP 02277 and MET 00639). Ivuna is the only CI chondrite analyzed in the present study. The 3 μm band center decreases with increasing alteration.

group, group 3 is the most altered group (before Ivuna), and group 2 is an intermediate group. The 3 μm band center decreases with increasing alteration. Group 1, which has 3 μm band centers at longer wavelength, is consistent with Fe-rich serpentine minerals, such as cronstedtite. Group 3, which has 3 μm band centers at shorter wavelength, is consistent with Mg-rich serpentine minerals, such as antigorite. Group 1 corresponds to petrologic subtypes ranging from 2.6 to 2.3 and lower MAIs that vary from 0.33 to 0.67, consistent with the low degree of alteration in this group. Group 3 has petrologic subtypes ranging from 2.2 to 2.1 and higher MAIs that vary from 0.90 to 1.04, consistent with the high degree of alteration in this group. Group 3 includes LAP 02277 with a subtype of 2.1, which has been classified as a CM1 (Russell et al. 2005). Group 2 represents the transition between Group 1 (least altered) and group 3 (most altered). MAC 02606 in group 2 has a very low MAI of 0.35, possibly because it contains unusually high concentrations of carbonates.

Most researchers accept that CM chondrites experienced alteration processes on or within their parent asteroids (e.g., McSween 1979a, 1987; Brearley 2006), although arguments for solar nebula alteration have also been presented (e.g., Metzler et al. 1992). CM parent body alteration has been described as occurring in four stages (Tomeoka et al. 1989): (1) formation of tochilinite by interaction of Fe metal (kamacite) with a S-bearing fluid (sulfide) that moved through cracks in chondrules and aggregates; (2) formation of phyllosilicates from Fe-rich matrix olivine, and "spinach" from mesostasis glasses in chondrules and aggregates; (3) formation of magnesium cronstedtite by interaction of Si (released from the alteration of olivine and pyroxene) with tochilinite, and formation of tochilinite-cronstedtite intergrowths; (4) while tochilinite continued to be consumed, magnesium cronstedtite increased its Mg and Si contents by interacting with existing serpentine to form Fe-serpentine, which then altered to form Mg-serpentine. Unlike the scale of Rubin et al. (2007), the scale of Browning et al. (1996) includes only the second part of the fourth stage of alteration (alteration of Fe-serpentine to Mg-serpentine). Hence, it is possible that the MAI parameter alone does not capture all the

petrologic parameters that are expressed by the diversity of the 3 μm band and by the complex and multistage aqueous alteration experienced by CM chondrites.

Organic Compounds and Magnetite in CM and CI Chondrites

The association of aqueous alteration with organic compounds and magnetite in carbonaceous chondrites has been reported in several studies (e.g., Bunch and Chang 1980; Tomeoka and Buseck 1985; Cronin and Chang 1993). The abundance of organics is probably related to the aqueous alteration process during which phyllosilicates enabled the adsorption and trapping of organic material through subsequent mineral growth (Pearson et al. 2002). Magnetite is also generally thought to be a product of parent body aqueous alteration (e.g., Kerridge et al. 1979), although arguments for solar nebula formation have also been presented (e.g., Jedwab 1971).

Aliphatic Organics

Our spectral investigation has revealed that aliphatic organics' features in group 2 and Ivuna develop into sharper and more pronounced features as heating proceeds. We also note that the organic spectral features become slightly inverted when measured under heating and vacuum conditions (e.g., MIL 07700). This could be due to some organics that adsorbed on the standard, and because spectra of the standard were measured only once at the start of each sample run.

The increase in observed spectral contrast of the organic features appears to be due to the removal of the spectrally masking effects of the adsorbed water. It seems from the spectrally detected aliphatic organic compounds in group 2, rather than the group 3, that abundant organics may be associated with mineral diversity in these groups (Fig. 6f). We suggest four possible explanations for the spectral appearance of organics in dry spectra in group 2 and Ivuna: (1) adsorbed water, before it is minimized by heating, spectrally masks organic features; (2) removal of adsorbed water compositionally altered the mix of organic compounds; (3) new organic compounds formed during heating; or (4) organics were deposited onto the sample or sample window from elsewhere in the vacuum system. We do not observe any new organic absorption features being created, nor any features decreasing in strength (relative to other C-H absorptions) that would be indicative of bulk compositional changes. Also, the sample holder is the warmest component in the system and thus not likely to "cold-trap" organics in the vacuum system. Hence, there appear to be no major changes in the organic compounds within the sample. This also means that the organic compounds appear stable during the heating and vacuum runs. Therefore, of the three suggested explanations, the first one is the most likely explanation for the appearance of organics in both group 2 and Ivuna.

Amino Acids

Among the organic compounds in carbonaceous chondrites are amino acids, which are building blocks of life (e.g., Botta and Bada 2002; Pizzarello et al. 2006). Relative concentrations of amino acids in carbonaceous chondrites have been used to understand the nature of aqueous alteration processes experienced on the parent body (e.g., Botta et al. 2007). Glavin et al. (2011) found that carbonaceous chondrites with higher degrees of aqueous alteration have lower abundance of amino acids, suggesting that alteration influenced their formation. Furthermore, Monroe and Pizzarello (2011) suggested that repeated aqueous alteration processes on parent bodies might have altered or destroyed the original organic inventory of carbonaceous chondrites.

The amino acids exhibit diversity in their molecular structures and concentrations among carbonaceous chondrites. Botta et al. (2007) found that the abundance of amino acids in CM1 chondrites is significantly lower than in CM2s. LAP 02277 (CM1), also studied here (group 3), shows a unique amino acid distribution that cannot be related to any of the other classes studied by Botta et al. (2007). In addition, Ehrenfreund et al. (2001) showed that the amino acids in CIs, including Ivuna, are distinct from those in CM2s, and suggested that these classes had different parent bodies and were processed under different physical and chemical conditions. Oxygen isotope analyses also showed that CI and CM chondrites were altered at different temperatures and water/rock ratios (Clayton and Mayeda 1984, 1999). It is therefore likely that CM and CI chondrites have had distinct organic precursor compounds and thus their parent bodies were different, in agreement with the results of Eiler and Kitchen (2004), who suggested that CI and CM meteorites represented alteration of distinct parent materials.

Changes of aliphatic organic compounds in CM and CI carbonaceous chondrites with heating above room temperature are not well documented, but Cronin and Pizzarello (1983) noted a change in amino acids. The abundance of some amino acids, such as β-alanine, increased, while the abundance of others, such as γ-aminobutyric acid, decreased. We found no N-H absorptions at approximately 3.1 μm in any of our spectra, nor any C-H absorptions specifically attributable to amino acids (Fig. 9).

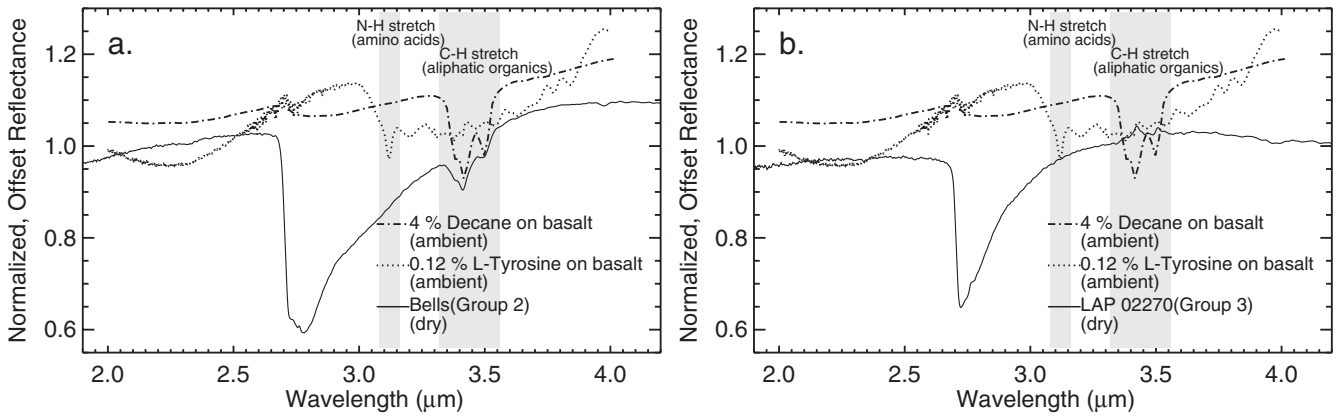

Fig. 9. a) Spectra of Bells (group 2), and of decane alkane (4%) and L-Tyrosine amino acid (0.12%) mixed with basalt (BHVO-2F). The 3.1 μm feature in Tyrosine spectrum is the N-H fundamental stretch of amino acids. If Tyrosine were in the meteorite sample with similar grain sizes, our detectability would be around 0.01 wt% (100 ppm). The absorptions at 3.4–3.5 μm are the C-H stretch of aliphatic organics. b) LAP 02770 (group 3) does not show the N-H stretch feature, nor the C-H stretch feature.

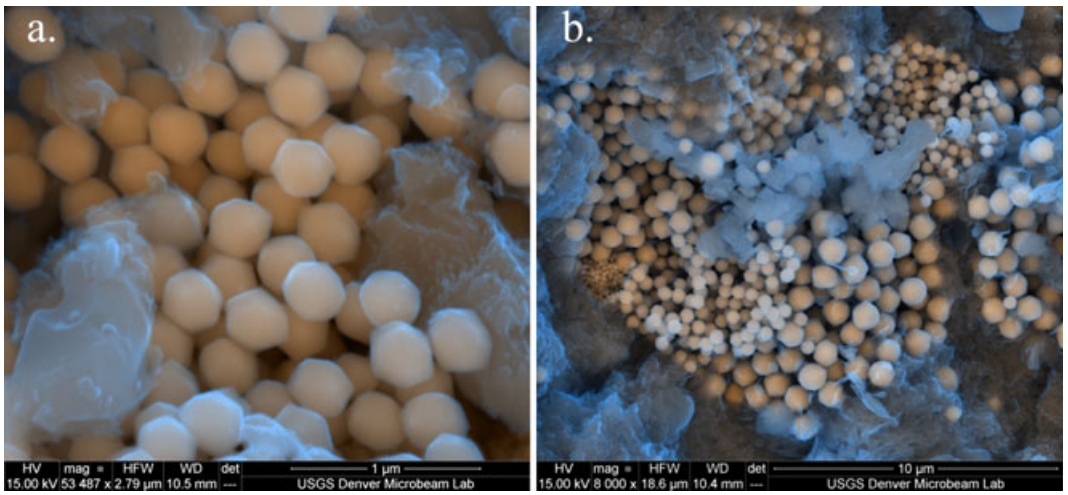

Fig. 10. a) Magnetite grains have been identified in Bells (group 2) as framboidal aggregates with polygonal morphology. b) Similar framboidal aggregates of magnetite grains have also been found in Ivuna (CI).

Magnetite

Magnetite has been identified in many CM and CI chondrites as framboidal aggregates with polygonal morphology (Jedwab 1971; Kerridge et al. 1979; Tomeoka and Buseck 1985). Magnetite was probably deposited in the matrix after the migration of Fe, S, and Ni from serpentine-tochilinite intergrowths (Tomeoka and Buseck 1985). McSween (1979a) also noted that magnetite abundance probably increases with alteration.

Using high-resolution SEM, we searched for magnetite in the ten CM and CI chondrites. We identified relatively abundant framboidal magnetite grains in three samples of group 2: Bells (subtype = 2.1 and MAI = 0.41), Cold Bokkeveld (subtype = 2.2 and MAI = 1.21), and MAC 02606 (subtype = 2.1 and MAI = 0.35), in addition to Ivuna. Framboidal magnetite grains found in CM chondrites are similar to those in Ivuna with the same polygonal morphology (Fig. 10). We also note that the broad adsorbed water feature at approximately 3.1 μm (in ambient spectra) and the sharper aliphatic organics feature (in dry spectra) are present in all of these four samples. This suggests that magnetite forms in an environment that enables the adsorption of water.

CONCLUSIONS

We have measured reflectance spectra of nine CM and one CI chondrites under dry and vacuum

conditions to minimize adsorbed water and mimic the space environment. These chondrites are classified into three groups, mainly on the basis of the 3 μm band center. Group 1, which is characterized by 3 μm band centers at 2.76–2.80 μm, is consistent with the endmember Fe-serpentine (cronstedtite). Group 3, which is characterized by 3 μm band centers at approximately 2.72 μm, is consistent with the endmember Mg-serpentine (antigorite). Group 2 represents an intermediate mineralogy between the two endmembers. Ivuna, which is the only CI chondrite analyzed in the present study, has a unique 3 μm band centered approximately 2.71 μm, consistent with lizardite and chrysotile. This diversity in the 3 μm band suggests distinct pre-terresterial aqueous alteration conditions for these chondrites, which provide clues to parent body alteration.

We applied two previously published alteration scales by Browning et al. (1996) and Rubin et al. (2007) to nine CM carbonaceous chondrites. We found good agreements between the petrologic and geochemical parameters, and spectral characteristics of these chondrites. The petrologic subtype in group 1 varies from 2.6 to 2.3 (least altered group) and in group 3 from 2.1 to 2.2 (most altered) in agreement with the spectral analyses. Geochemical analysis of matrix also shows that QUE 97990 (group 1), which is the least altered sample, is consistent with cronstedtite. More spectral analyses on the intermediate phases between endmembers Fe-serpentine and Mg-serpentine are needed to better characterize the mineralogy in group 2.

For group 2 and Ivuna, the organic absorptions became more pronounced at elevated temperatures, possibly because the adsorbed water, before it is minimized by heating, spectrally masks the organic feature. Hence, both group 2 and Ivuna are characterized by adsorptive surfaces. Magnetite abundance is relatively higher in chondrites that show the broad adsorbed water feature at approximately 3.1 μm (in ambient spectra) and the pronounced aliphatic organics feature (in dry spectra). These results suggest that magnetite forms in an environment that enables adsorption of volatiles. CM and CI chondrite spectra show no evidence for amino acids, probably due to their low abundance. The presence of aliphatic organics and magnetite in group 2 and Ivuna further supports that these meteorites experienced moderate aqueous alteration processes.

This study has direct implications for the interpretation of ground-based telescope spectra of outer Main Belt asteroids (Takir and Emery 2012). The consistency between petrologic and geochemical parameters, which were determined using electron microprobe and microscope analyses, and the spectral properties of CM meteorites indicates that distinct parent body aqueous alteration environments can be distinguished using reflectance spectroscopy. High-quality ground-based telescopic observations of outer Main Belt asteroids can potentially reveal not just whether an asteroid is hydrated, but also the nature and degree of its aqueous alteration.

This study may also have some implications for: (1) the interpretation of the dark material on Vesta, which is thought to be from the infall of carbonaceous volatile-rich material (McCord et al. 2012); (2) the interpretation of spectra of Ceres that will be visited by the Dawn spacecraft in 2015; (3) the interpretation of spectra and the returned sample from the carbonaceous asteroid Bennu that will be visited by the OSIRIS-REx spacecraft (Lauretta et al. 2010); and (4) the interpretation of the dark material in the Saturn system (Clark et al. 2012).

Acknowledgments—We are grateful for thoughtful reviews by Janice Bishop and Ralph Milliken. We thank Allan Patchen for assistance with the electron microprobe, Bill Deane and Michael DeAngelis for assistance with serpentine preparation and XRD measurements, Jeff Moersch for access to the ASD spectrometer, Yali Lu for assistance with Raman spectra measurements, Heather Lowers for assistance with the SEM measurements, and Genesis Berlanga for assistance with reflectance spectra measurements. This work was partly supported by NASA Cosmochemistry grant NNX13AH86G to HYM, NASA Planetary Astronomy grant NNX08AV93G to JPE, and the NASA Cassini mission to Saturn, VIMS team to RNC.

Editorial Handling—Dr. Carle Pieters

REFERENCES

Beck P., Quirico E., Montes-Hernandez G., Bonal L., Bollard J., Orthous-Daunay F. R., Howard K. T., Schmitt B., Brissaud O., Deschamps F., Wunder B., and Guillot S. 2010. Hydrous mineralogy of CM and CI chondrites from infrared spectroscopy and their relationship with low albedo asteroids. *Geochimica et Cosmochimica Acta* 74:4881–4892.

Bell J. F., Davis D. R., Hartmann W. K., and Gaffey M. J. 1989. Asteroids: The big picture. In *Asteroid II*, edited by Binzel R. P., Gehrels T., and Matthews M. S. Tucson, Arizona: The University of Arizona Press. pp. 921–945.

Botta O. and Bada J. L. 2002. Extraterrestrial organic compounds in meteorites. *Survey of Geophysics* 23:411–465.

Botta O., Zita M., and Ehrenfreund P. 2007. Amino acids in Antarctic CM1 meteorites and their relationship to other

carbonaceous chondrites. *Meteoritics & Planetary Science* 42:81–92.

Brearley A. J. 1997. Phyllosilicates in the matrix of the unique carbonaceous chondrite, LEW 85332 and possible implications for aqueous alteration of CI chondrites. *Meteoritics & Planetary Science* 32:377–388.

Brearley A. J. 2006. The action of water. In *Meteorites and the early solar system II*, edited by Lauretta D. and McSween H. Y. Tucson, Arizona: The University of Arizona Press. pp. 587–624.

Browning L. B., McSween H. Y., and Zolensky M. E. 1996. Correlated alteration effects in CM carbonaceous chondrites. *Geochimica et Cosmochimica Acta* 60:2621–2633.

Browning L. B., McSween H. Y., and Zolensky M. E. 2000. On the origin of rim textures surrounding anhydrous silicate grains in CM carbonaceous chondrites. *Meteoritics & Planetary Science* 35:1015–1023.

Bunch T. E. and Chang S. 1980. Carbonaceous chondrite phyllosilicates and light element geochemistry as indicators of parent body processes on surface conditions. *Geochimica et Cosmochimica Acta* 44:1543–1577.

Burns R. G. 1993. Origin of electronic spectra in minerals in the visible to near-infrared region. In *Topics in remote sensing 4: Remote geochemical analysis: Elemental and mineralogical composition*, edited by Pieters C. M. and Englert P. A. J. Cambridge, UK: Cambridge University Press. pp. 3–29.

Clark R. N. 1983. Spectral properties of mixtures of montmorillonite and dark carbon grains: Implications for remote sensing minerals containing chemically and physically adsorbed water. *Journal of Geophysical Research* 88:10635–10644.

Clark R. N. and Roush T. L 1984. Reflectance spectroscopy: Quantitative analysis techniques for remote sensing applications. *Journal of Geophysical Research* 89:6329–6340.

Clark R. N., King T. V. V., Klewja M., Swayze G. A., and Vergo N. 1990. High spectral resolution reflectance spectroscopy of minerals. *Journal of Geophysical Research* 95:12653–12680.

Clark R. N., Swayze G. A., Livo K. E., Kokaly R. F., King T. V. V., Dalton J. B., Vance J. S., Rockwell B. W., Hoefen T., and McDougal R. R. 2002. Surface reflectance calibration of terrestrial imaging spectroscopy data: A tutorial using AVIRIS. Proceedings, XXth Airborne Earth Science Workshop, JPL Publication 02-1.

Clark R. N, Swayze G. A., Wise R., Livo E., Hoefen T., Kokaly R., and Sutley S. J. 2007. *USGS digital spectral library splib06a*, Data Series, 231, U.S. Geological Survey, Reston, VA. (http://speclab.cr.usgs.gov/spectral.lib06).

Clark R. N., Curchin J. M., Hoefen T. M., and Swayze G. A. 2009. Reflectance spectroscopy of organic compounds I: Alkanes. *Journal of Geophysical Research* 114:E03001.

Clark R. N., Pearson N., Takir D., Emery J. P., McSween H. Y., Cruikshank D. P., and Hendrix A. R. 2012. Nano-iron on outer solar system satellites, implications for space weathering (abstract #53B-05). 45th American Geophysical Union Fall meeting.

Clayton R. N. and Mayeda T. K. 1984. The oxygen isotope record in Murchison and other carbonaceous chondrites. *Earth and Planetary Science Letters* 67:151–161.

Clayton R. N. and Mayeda T. K. 1999. Oxygen isotope studies of carbonaceous chondrites. *Geochimica et Cosmochimica Acta* 63:2089–2104.

Cloutis E. A., Gaffey M. J., Jackowski T. L., and Reed K. L. 1986. Calibrations of phase abundance, composition, and particle size distribution for olivine-orthopyroxene mixtures from reflectance spectra. *Journal of Geophysical Research* 91:11,641–11,653.

Cronin J. R. and Chang S. 1993. Organic matter in meteorites: Molecular and isotopic analyses of the Murchison meteorite. In *Chemistry of life's origins*, edited by Greenburg J. M. and Pirronello V. Dordrecht, the Netherlands: Kluwer. pp. 209–258.

Cronin J. R. and Pizzarello S. 1983. Amino acids in meteorites. *Advances in Space Research* 9:5–18.

Ehrenfreund P., Glavin D. P., Botta O., Cooper G., and Bada J. L. 2001. Extraterrestrial amino acids in Orgueil and Ivuna: Tracing the parent body of Cl type carbonaceous chondrites. *Proceedings of the National Academy of Sciences* 98:2138–2141.

Eiler J. M. and Kitchen N. 2004. Hydrogen isotope evidence for the origin and evolution of the CM chondrites. *Geochimica et Cosmochimica Acta* 68:1395–1411.

Gaffey M. J., Burbine T. H., and Binzel R. P. 1993. Asteroid spectroscopy: Progress and perspectives. *Meteoritics*, 28:161–187.

Glavin D. P., Callahan M. P., Dworkin J. P., and Elsila J. E. 2011. The effects of parent body processes on amino acids in carbonaceous chondrites. *Meteoritics & Planetary Science* 45:1948–1972.

Hibbitts C. A., Hagaman S., and Greenspon A. 2012. The adsorption of gases onto refractory materials: CO_2 onto clays and their relevance to the icy Galilean satellites (abstract #2400). 43rd Lunar and Planetary Science Conference. CD-ROM.

Howard K. T., Benedix G. K., Bland P. A., and Cressey G. 2009. Modal mineralogy of CM2 chondrites by X-ray diffraction (PSD-XRD). Part 1: Total phyllosilicate abundance and the degree of aqueous alteration. *Geochimica et Cosmochimica Acta* 73:4576–4589.

Howard K. T., Benedix G. K., Bland P. A., and Cressey G. 2011. Modal mineralogy of CM chondrites by X-ray diffraction (PSD-XRD): Part 2. Degree, nature and settings of aqueous alteration. *Geochimica et Cosmochimica Acta* 75:2735–2751.

Jedwab J. 1971. La magnetite de la meteorite d'orgueil vu au microscope electronic a balayage. *Icarus* 15:319–340.

Kerridge J. F., Mackay A. L., and Boynton W. V. 1979. Magnetite in CI carbonaceous meteorites—Origin by aqueous activity on a planetesimal surface. *Science* 205:395–397.

Larson H. P., Feierberg M. A., Fink U., and Smith H. A. 1979. Remote spectroscopic identification of carbonaceous chondrite mineralogies: Applications to Ceres and Pallas. *Icarus* 39:257–271.

Lauretta D. S., Drake M. J., Binzel R. P., Campins H., Chesley S. R., Clark B. E., Delbo M., Emery J. P., Hergenrother C. W., Nolan M. C., Scheeres D. J., and OSIRIS-REx team. 2010. Asteroid 101955 1999 RQ36: Optimum target for an asteroid sample return mission (abstract #5153). *Meteoritics and Planetary Science Supplement*.

Lebofsky L. A. 1980. Infrared reflectance spectra of asteroids: A search for water of hydration. *The Astronomical Journal* 85:573–585.

Lee M. 1993. The petrography, mineralogy and origins of calcium sulphate within the Cold Bokkeveld CM carbonaceous chondrite. *Meteoritics* 28:53–62.

McCord T. B., Li J.-Y., Combe J.-P.. McSween H. Y., Jaumann R., Reddy V, Tosi F., Williams D. A., Blewett D. T., Turrini D., Palomba E., Pieters C. M., De Sanctis M. C., Ammannito E., Capria M. T., Le Corre L., Longobardo A., Nathues A., Mittlefehldt D. W., Schröder S. E., Hiesinger H., Beck A. W., Capaccioni F., Carsenty U., Keller H. U., Denevi B. W., Sunshine J. M., Raymond C. A., and Russell C. T. 2012. Dark material on Vesta from the infall of carbonaceous volatile-rich material. *Nature* 491:83–86.

McSween H. Y. 1979a. Alteration in CM carbonaceous chondrites inferred from modal and chemical variations in matrix. *Geochimica et Cosmochimica Acta* 43:1761–1770.

McSween H. Y. 1979b. Are carbonaceous chondrites primitive or processed? A review. *Reviews of Geophysics and Space Physics* 17:1059–1078.

McSween H. Y. 1987. Aqueous alteration in carbonaceous chondrites: Mass balance constraints on matrix mineralogy. *Geochimica et Cosmochimica Acta* 51:2469–2477.

Metzler K., Bischoff A., and Stoffler D. 1992. Accretionary dust mantles in CM chondrites: Evidence for solar nebula processes. *Geochimica et Cosmochimica Acta* 56:2873–2897.

Miyamoto M. and Zolensky M. E. 1994. Infrared diffuse reflectance spectra of carbonaceous chondrites: Amount of hydrous minerals. *Meteoritics* 29:849–853.

Monroe A. A. and Pizzarello S. 2011. The soluble organic compounds of the Bells meteorite: Not a unique or unusual composition. *Geochimica et Cosmochimica Acta* 75:7585–7595.

Osawa T., Kagi H., Nakamura T., and Noguchi T. 2005. Infrared spectroscopic taxonomy for carbonaceous chondrites from speciation of hydrous components. *Meteoritics & Planetary Science* 40:71–86.

Pearson V. K., Kearsley A. T., Sephton M. A., and Glimour I. 2002. Organic-inorganic spatial relationships in carbonaceous chondrites (abstract #1311). 33rd Lunar and Planetary Science Conference. CD-ROM.

Pizzarello S., Cooper G. W., and Flynn G. J. 2006. The nature and distribution of the organic material in carbonaceous chondrites and interplanetary dust particles. In *Meteorites and the early solar system II*, edited by Lauretta D. and McSween H. Y. Tucson, Arizona: The University of Arizona Press. pp. 625–651.

Pouchou J. L. and Pichoir F. 1987. In *Basic expression of "PAP" computation for quantitative EPMA*. In Proceedings of the 11th ICXOM, edited by Brown J. D. and Packwood R. H. London, Ontario: University of Western Ontario. pp. 249–253.

Rivkin A. S., Howell E. S., Vilas F., and Lebofsky L. A. 2002. Hydrated minerals on asteroids: The astronomical record. In *Asteroids III*, edited by Bottke W. F., Jr., Cellino P., Paolicch P., and Binzel R. P. Tucson, Arizona: The University of Arizona Press. pp. 235–253.

Rivkin A. S., Davies J. K., Johnson J. R., Ellison S. L., Trilling D. E., Brown R. H., and Lebofsky L. A. 2003. Hydrogen concentrations on C-class asteroids derived from remote sensing. *Meteoritics & Planetary Science* 38:1383–1398.

Rubin A. J., Trigo-Rodríguez J. M., Huber H., and Wasson J. T. 2007. Progressive aqueous alteration of CM carbonaceous chondrites. *Meteoritics & Planetary Science* 71:2361–2382.

Russell S. S., Zolensky M., Righter K., Folco L., Jones R., Connolly H. C., Grady M. M., and Grossman J. N. 2005. The Meteoritical Bulletin, No. 89. *Meteoritics & Planetary Science* 40:A201–A263.

Salisbury J. W., Walter L. S., Vergo N., and D'Aria D. 1991. *Infrared (2.1–25 μm) spectra of minerals*. Baltimore: Johns Hopkins University Press. 267 p.

Sato K., Miyamoto M., and Zolensky M. E 1997. Absorption bands near three micrometers in diffuse reflectance spectra of carbonaceous chondrites: Comparison with asteroids. *Meteoritics & Planetary Science* 32:503–507.

Sunshine J. M., Farnham T. L., Feaga L. M., Groussin O., Merlin F., Milliken R. E, and A'Hearn M. F. 2009. Temporal and spatial variability of lunar hydration as observed by the Deep Impact spacecraft. *Science* 326:565–568.

Takir D. and Emery J. P. 2012. Outer Main Belt asteroids: Identification and distribution of four 3-μm spectral groups. *Icarus* 219:641–654.

Tomeoka K. and Buseck P. R 1985. Indicators of aqueous alteration in CM carbonaceous chondrites: Microtextures of a layered mineral containing Fe, S, O and Ni. *Geochimica et Cosmochimica Acta* 49:2149–2163.

Tomeoka K., McSween H. Y., and Buseck P. R 1989. Mineralogical alteration of CM carbonaceous chondrites: A review. *Proceedings of the National Institute of Polar Research Symposium* 2:221–234.

Van Schmus W. R. and Wood J. A. 1967. A chemical-petrologic classification for the chondritic meteorites. *Geochimica et Cosmochimica Acta* 31:747–765.

Velbel M. A. and Palmer E. E. 2012. Fine-grained serpentine in CM2 carbonaceous chondrites and its implications for the extent of aqueous alteration on the parent body: A review. *Clays and Clay Minerals* 59:416–432.

Vilas F. and Gaffey M. J. 1989. Phyllosilicate absorption features in main-belt and outer-belt asteroids from reflectance spectroscopy. *Science* 246:790–792.

Wang A., Freeman J. J., Jolliff B. L., and Chou I. 2006. Sulfates on Mars: A systematic Raman spectroscopic study of hydration states of magnesium sulfates. *Geochimica et Cosmochimica Acta* 70:6118–6135.

Weidner V. R. and Hsia J. J. 1981. Reflection properties of pressed polytetrafluoroethylene powder. *The Journal of the Optical Society of America* 71:856–859.

Zaikowski A. 1979. Infrared-spectra of the Orgueil (C-1) chondrite and serpentine minerals. *Geochimica et Cosmochimica Acta* 3:943–945.

Zolensky M. E. and McSween H. Y. 1988. Aqueous alteration. In *Meteorites and the early solar system*, edited by Kerridge F. and Mattews M. Tucson, Arizona: The University of Arizona Press. pp. 114–143.

Zolensky M. E., Barret R., and Browning L. B. 1993. Mineralogy and composition of matrix and chondrule rims in carbonaceous chondrites. *Geochimica et Cosmochimica Acta* 57:3123–3148.

SUPPORTING INFORMATION

Additional supporting information may be found in the online version of this article:

Fig. S1: Spectra of CM and CI carbonaceous chondrites measured at different temperatures and pressures. Several spectra were averaged for each temperature step.

Fig. S2: Ternary diagrams of matrix compositions in nine CM chondrites and one CI carbonaceous chondrite.